Rare Metal Materials and Engineering
Volume 49, Issue 12, December 2020
Available online at www.rmme.ac.cn

Science Press

Cite this article as: Rare Metal Materials and Engineering, 2020, 49(12): 4023-4030.

ARTICLE

Microstructure and Mechanical Properties of Selective Laser Melted Pure Tantalum Using Radio Frequency Plasma Spheroidized Powder

Shi Qi[1,2,3], Mao Xinhua[1,2,3], Tan Chong[1,2,3], Ding Chao[1,2,3], Liu Xin[1,2,3]

[1] Institute of Materials and Processing, Guangdong Academy of Sciences, Guangzhou 510650, China; [2] National Engineering Research Center of Powder Metallurgy of Titanium & Rare Metals, Guangzhou 510650, China; [3] Key Laboratory of Metal Strengthening and Toughening Technology and Application of Guangdong, Guangzhou 510650, China

Abstract: Spherical tantalum powder fabricated by radio frequency plasma spheroidization system was used for selective laser melting (SLM) densification. Through optimizing the processing parameters, the fully dense Ta sample was obtained at the scanning speed of 650 mm/s and the laser power of 240 W. Results show that attributed to the high sphericity, the Ta samples perform better densification behavior and surface quality. Microstructure characterization shows that equiaxed grains and columnar structure are present in the top and side views, respectively. The EBSD results reveal a <111> preferred orientation along the building direction. The maximum microhardness and the ultimate tensile strength reach 2962 MPa and 697 MPa, respectively. A significantly improved ductility with an elongation of 28.5% is achieved for the dense sample.

Key words: selective laser melting; spherical tantalum powder; densification; texture; mechanical properties

Tantalum (Ta) has been considered as a promising biomaterial in medical applications because of the high corrosion resistance and extraordinary biocompatibility[1-5]. Stiehler et al[6] reported that the attachment, proliferation and osteogenic differentiation of osteoprogenitor cells on Ta are better than those on the titanium alloy, which makes Ta is commonly used as the bone implant. In addition, Ta coating[7-9] and Ta-content alloys[10-12] are also employed in biomedical implant fields. However, the high melting temperature (2996 °C), difficult-to-work properties and high cost impede its further usage. In recent years, the development of additive manufacturing technology provides a new approach to fabricate porous and dense Ta parts[4,13-15]. The selective laser melting (SLM), as an additive manufacturing technique, is capable of fabricating 3D parts with complex geometries based on a layer-by-layer incremental manufacturing concept[16,17]. Zhou et al[18] suggested that the microhardness and tensile strength of the SLMed Ta parts can be significantly improved by optimizing processing parameters. Nevertheless, the elongation of the obtained samples is only 2% due to the remained micropores, which are highly related to the employed hydrogenation-dehydrogenation Ta powder with irregular shape. In this study, spherical Ta powder fabricated by radio frequency plasma spheroidization system was used, and a comprehensive investigation on the densification behavior, microstructure and mechanical properties were carried out.

1 Experiment

The raw material used in this study was spherical Ta powder fabricated by the radio frequency plasma spheroidization system (TEKNA-40 kW). As shown in Fig.1a, the powders are mostly spherical, and a few satellite particles can

Received date: December 11, 2019
Foundation item: Domestic First-class Research Institute Project of Guangdong Academy of Sciences (2019GDSYL-0302017); Collaborative Innovation and Platform Construction Project of Guangdong Province (2017A050501024, 2017A050503004); Public Research and Capacity Building Project of Guangdong Province (2017A070701029); Natural Science Foundation of Guangdong Province (2018A030313127); Guangdong Academy of Sciences Project and Development (2018GDASCX-0961); Guangzhou Science and Technology Program (201906040007)
Corresponding author: Liu Xin, Ph. D., Professor, Institute of Materials and Processing, Guangdong Academy of Sciences, Guangzhou 510650, P. R. China, Tel: 0086-20-61086128, E-mail: shaneliu118@163.com

be found under a higher magnification (Fig.1b). As shown in Fig.2, the powder particles have a size distribution of D_{10}=19.1 μm, D_{50}=29.2 μm, and D_{90}=45.8 μm. The apparent density and tap density of the powders were 9.450 and 10.513 g/cm^3, respectively. The flowability measured by Hall flowmeter was 5.78 s/50 g. The oxygen content was 481 μL/L.

The sample preparation was performed in a selective laser melting apparatus (EOS M290), on a Ti-6Al-4V substrate plate preheated at 100 °C under argon atmosphere. The angle of the scanning direction between the successive layers was 67°. The process parameters used in this experiment are presented in Table 1: laser power (P) varying from 160 W to 240 W, scanning speed (v) of 650 and 750 mm/s, and the layer thickness (d) and the hatch distance (h) of 20 and 80 μm, respectively. The corresponding volumetric laser energy density (E) was calculated using Eq.(1).

$$E=P/vdh \quad (1)$$

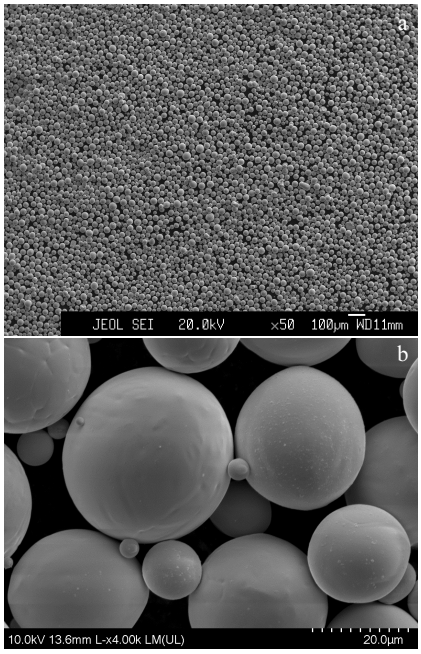

Fig.1 SEM images of Ta powder

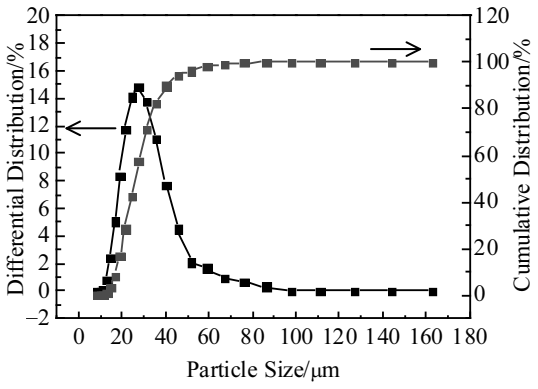

Fig.2 Particle size distribution of raw Ta powder

Table 1 Processing parameters for Ta sample preparation

Sample	Laser power, P/W	Scanning speed, v/mm·s^{-1}	Layer thickness, d/μm	Hatch distance, h/μm	Energy density, E/J·mm^{-3}
S1	160	650	20	80	153.83
S2	200	650	20	80	192.31
S3	240	650	20	80	230.77
S4	160	750	20	80	133.33
S5	200	750	20	80	166.67
S6	240	750	20	80	200.00

The density of the SLMed Ta samples was measured by Archimedes method, and the theoretical density of 16.6 g/cm^3 was used for the relative density calculation. The surface roughness was measured by a surface roughness tester (HANDYSURF E-35B-AICON). The phase constitution was identified using X-ray diffractometer (XRD, Rigaku D/MAX-RC) with a Cu Kα radiation. A scanning electron microscope (SEM, JEOL JXA-8100) equipped with Oxford HKL Nordly Max EBSD accessory was employed for microstructure observation and local texture investigation. Vickers microhardness was measured on the mechanically polished specimens using Zwick-Roell Zhμ Vickers hardness tester. The tensile tests were carried out using a Zwick/Roell Z250 testing machine.

2 Results and Discussion

2.1 Relative density and surface roughness

Fig.3 shows the relationship between the relative density and the laser energy density. It is clear that when the scanning speed is fixed, the relative density of the SLMed Ta samples increases with the energy density, and the maximum value of 99.96% is achieved when the scanning speed is 650 mm/s and the laser power is 240 W (sample S3 in Table 1). The surface morphology micrographs and the corresponding high magnified images are presented in Fig.4, where the laser scanning tracks can be clearly discerned, and the width of the tracks is ~85 μm. At relatively low laser power (P=160 W), obvious pores can be observed at the junction of ripples, as indicated by arrows in Fig.4a′ and 4d′. This is caused by insufficient laser energy input, which leads to higher liquid viscosity and shorter liquid lifetime[19]. In comparison with Fig.4a′, the increase in the scanning speed during the SLM process of the sample shown in Fig.4d′ results in not only lower energy density but also higher temperature gradient, leading to the higher surface tension gradient and the enhanced Maragoni convection, and hence the higher porosity. At higher laser powers (200 and 240 W), the pores are eliminated attributed to the enough energy input, and the resultant relative density is generally higher than 99.5%.

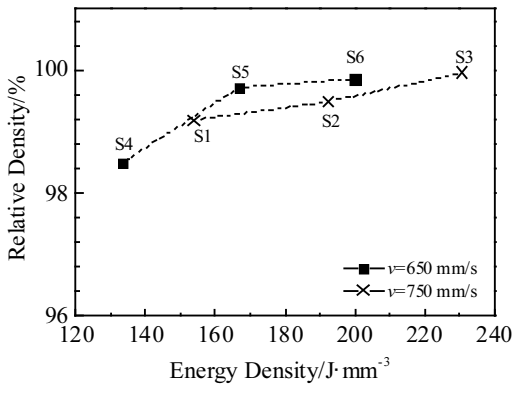

Fig.3 Relative density variations with the laser energy density

Compared to the previous study carried out by Zhou et al[18], a significant improvement in densification is obtained in the current research. In their work, the maximum relative density of 97.96% was achieved under a relatively high energy density of 434.78 J/mm^3 (P=300 W, v=100 mm/s, d=30 μm and h=230 μm) at both higher and lower scanning speeds, and irregular shape micropores are found. According to their explanation, the micropores formed at a relatively high scanning speed (v=200 mm/s) and a low energy density (181.15 J/mm^3) are suggested to be attributed to the discontinuous scanning tracks[19]. However, in the current research, even at the higher scanning speed (750 mm/s) and attendant lower energy density (133.33 J/mm^3), the relative density of sample S4 can be achieved over 98%. This improved SLM densification can be attributed to the spherical raw Ta powder produced by radio

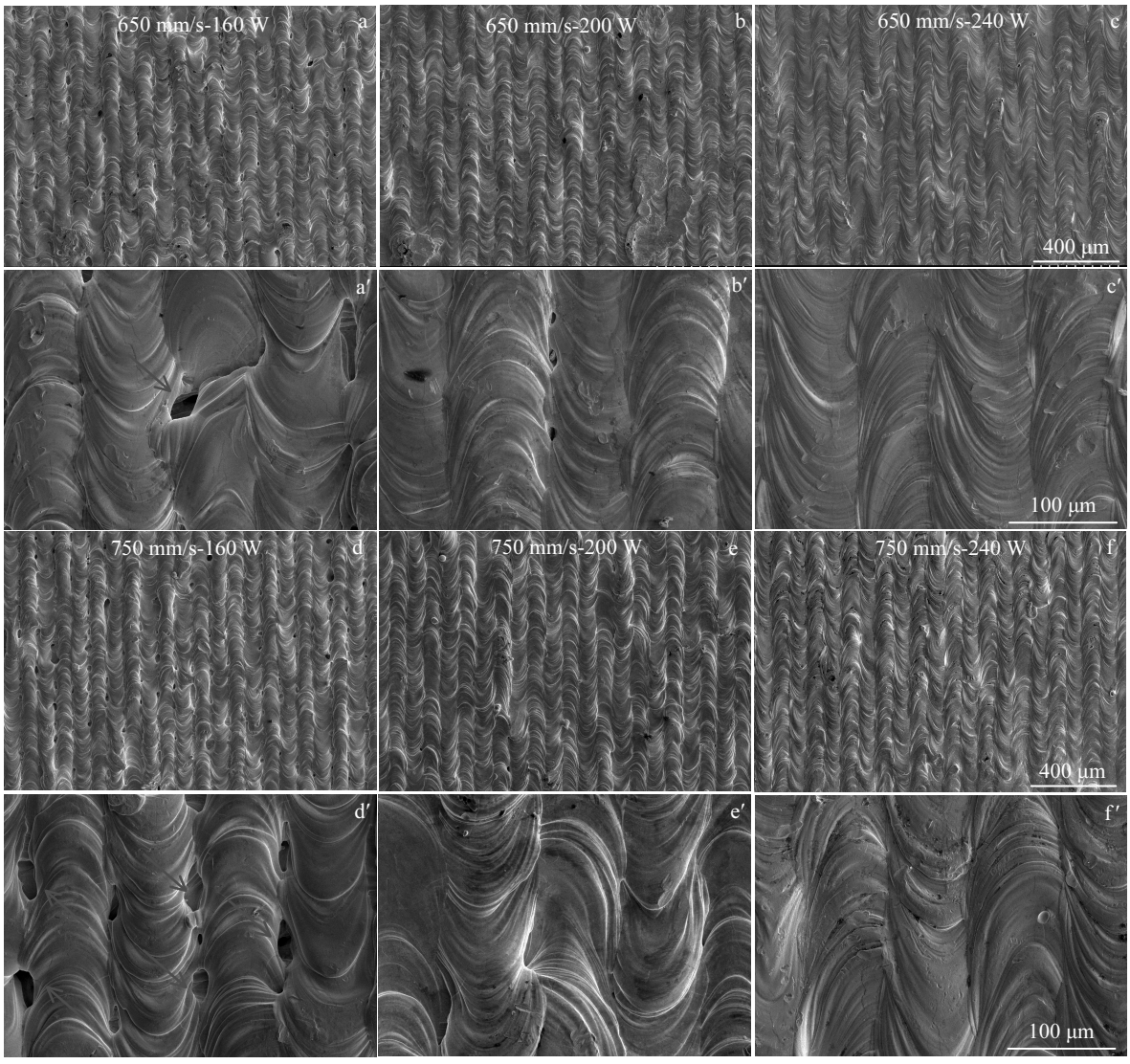

Fig.4 Surface morphologies of SLMed Ta samples (a~f) and corresponding high magnified images (a′~f′) under different processing parameters: (a, a′) 650 mm/s, 160 W; (b, b′) 650 mm/s, 200 W; (c, c′) 650 mm/s, 240 W; (d, d′) 750 mm/s, 160 W; (e, e′) 750 mm/s, 200 W; (f, f′) 750 mm/s, 240 W

frequency plasma spheroidization system, instead of hydrogenation/ dehydrogenation of Ta powder with irregular morphology. The high sphericity leads to better powder flowability and higher packing density during SLM process. As reported by Lee et al[20], an increase in packing density can facilitate elimination of the discontinuous molten pool and produce denser parts. In addition, a large number of previous studies indicate that lower powder packing density enhances fluid convection driven downwards by gravity[20-23], which can further aggravate the instability of the molten pool and hence the balling defects.

As shown in Fig.5, the surface roughness decreases with the energy density. It is known that the processing parameters, including the laser power, scanning speed and overlap ratio, have strong influences on the surface roughness. According to Fig.4, it can be seen that the neighboring tracks are overlapped and the overlap ratio can be calculated using Eq.(2):

$$\delta=(1-L/D)\times 100\% \quad (2)$$

where δ is the overlap ratio, L is the hatch distance and D is the laser spot diameter (D=100 μm in this case). Thus, the overlap ratio in the current study equals to 20%. According to the research carried out by Qin et al[24], when the overlap ratio is less than 50%, the surface roughness value decreases with the laser power density, which is consistent with the trend in Fig.5. This phenomenon can be explained by the fact that the increase in the energy density prolongs the lifetime of the molten pool, which also increases the fluidity of the molten, and hence the surface smoothness.

2.2 Phase, microstructure and texture

The phase identification of the SLMed Ta samples was performed using XRD. As revealed in Fig.6, single Ta phase with body center cubic (bcc) crystalline structure is present in the SLMed Ta parts. In comparison with raw Ta powder, the diffraction peaks are broadened. As shown in Fig.6b and 6d, with the increase in the energy density, the (110) peaks tend to shift to higher angles because of the increase in the residual stress[25]. However, it is noteworthy that the (110) peak of sample S4 (E=133.33 J/mm^3) is slightly on the right side of that of sample S1 (E=153.83 J/mm^3). This might be related to the higher scanning speed, resulting in higher temperature gradient, and hence the residual stress[26].

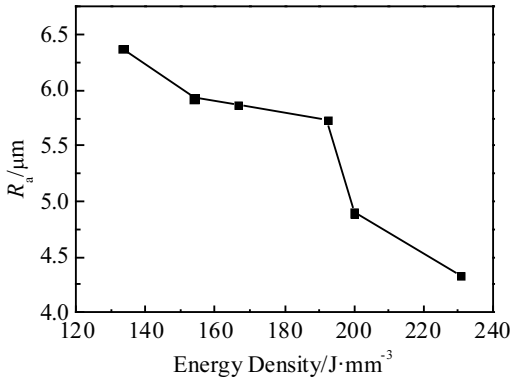

Fig.5 Effect of energy density on the surface roughness R_a

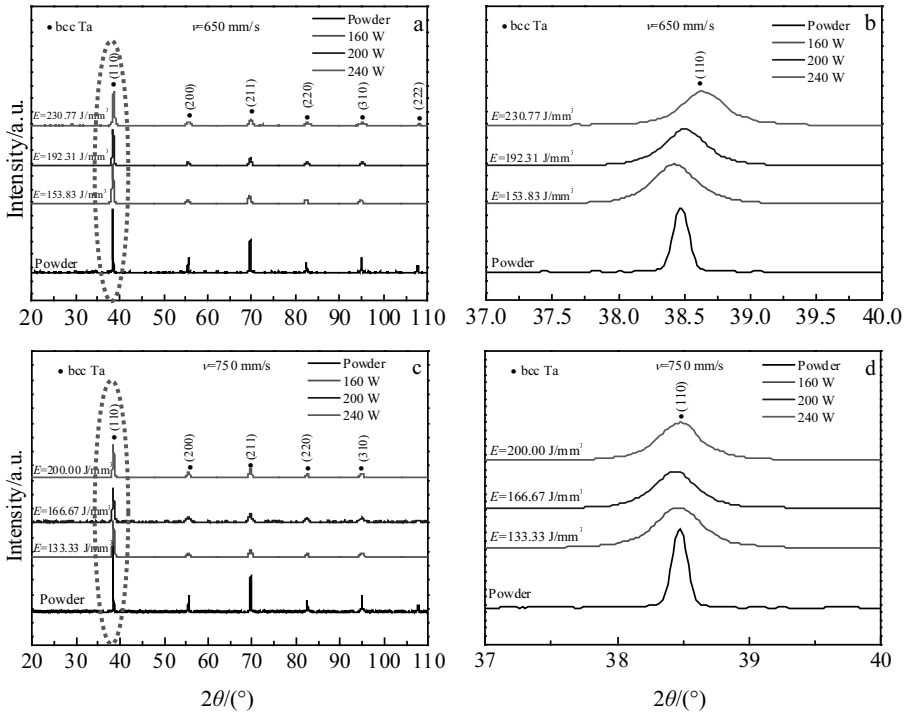

Fig.6 XRD patterns of SLMed Ta samples at different scanning speeds: (a, b) v=650 mm/s and (c, d) v =750 mm/s

The cross-sectional microstructures of the SLMed Ta samples are shown in Fig.7. As indicated by the circles in Fig.7a, at the scanning speed of 650 mm/s and laser power of 160 W, micropores are observed. When the scanning speed increases to 750 mm/s, the number of micropores increases (Fig.7d). With the increase of the laser power, few micropore is found. The observation is consistent with the relative density variation.

In order to further investigate the microstructure, EBSD analysis is carried out on the top plane of the SLMed Ta sample. The blue lines in Fig.8a denote the high angle grain boundaries

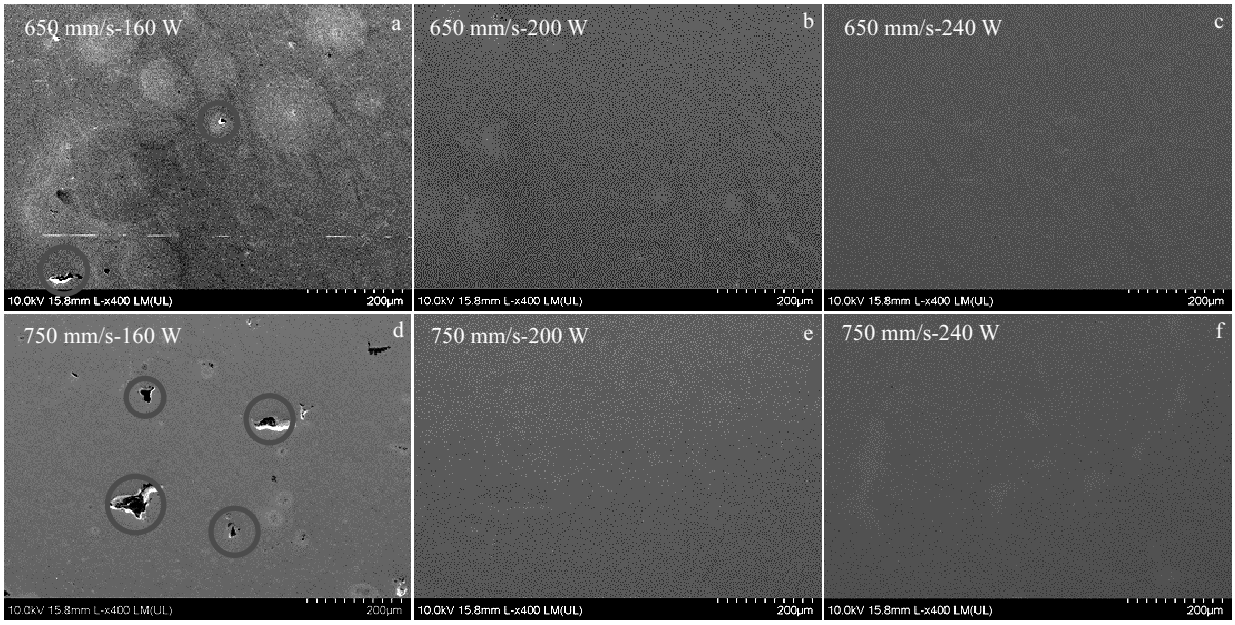

Fig.7 SEM images of the SLMed samples processed under different conditions: (a) *v*=650 mm/s, *P*=160 W; (b) *v*=650 mm/s, *P*=200 W; (c) *v*=650 mm/s, *P*=240 W; (d) *v*=750 mm/s, *P*=160 W; (e) *v*=750 mm/s, *P*=200 W; (f) *v*=750 mm/s, *P*=240 W

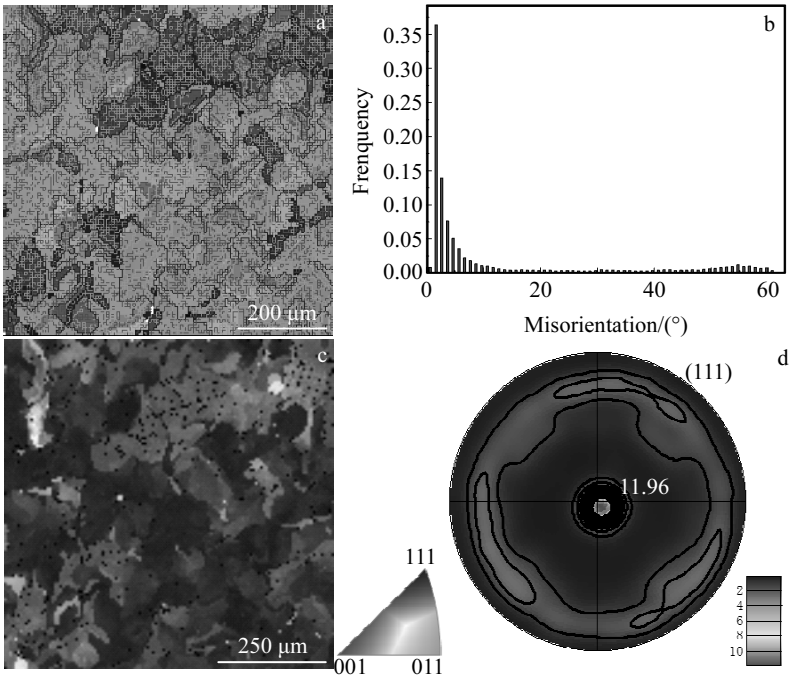

Fig.8 EBSD analysis of the top-view of the SLMed Ta sample: (a) misorientation distribution map of grain boundaries, (b) grain boundary misorientation histogram, (c) EBSD inverse pole figure image, and (d) (111) pole figure

(>15°). The equiaxed grains are found in an approximately hexagonal pattern, and the average grain size is ~80 μm, which indicates that the grains are confined to the scanning tracks. As revealed in Fig.8b, the fraction of high angle grain boundaries is ~22.8%. The EBSD-derived inverse pole figure (Fig.8c) shows that the <111> crystal direction of most grains is aligned with the building direction (BD) and some <001> crystal components are also present. The pole figure (Fig.8d) indicates a strong texture of <111>//BD. According to the previous studies[14,27], the texture evolution is significantly affected by the heat flux direction alternation, which causes the rotation of cubic crystals. In the current experiment, the laser paths are rotated by 67°, the competitive grain selection is pronounced, and thus an intensive texture forms[27]. Fig.9 shows the EBSD inverse pole figure image and the corresponding pole figure of the side-view for the same sample. The vertical columnar structure is found along the building direction, and different crystallographic directions are present on the side-view, although there is a preferred orientation along the scanning direction (SD).

2.3 Mechanical properties

Fig.10 shows the microhardness variation of the SLMed Ta samples processed using different parameters. When the laser power is fixed at 160 W (S1 and S4) and 200 W (S2 and S5), the microhardness reduces with the decrease in scanning speed, because the lower scanning speed leads to larger heat accumulation, and hence more serious grain coarsening[28]. However, it should be noted that the peak microhardness value of 2962 MPa is obtained when the laser power is 240 W and the scanning speed is 650 mm/s, which is comparable to the pure Ta subjected to severe plastic deformation[29]. This might be ascribed to the improvement of densification. As reported by Huang et al[29], the pure tantalum after an annealing treatment with an average grain size of ~60 μm has a Vickers hardness of ~870 MPa. The significant enhancement in microhardness can be attributed to the residual stress in the SLMed Ta sample.

Fig.11 shows the variation of the tensile strength and elongation δ with the energy density. It can be observed that at a fixed scanning speed, the ultimate tensile strength (σ_b) slightly increases with the energy density. In contrast to the previous

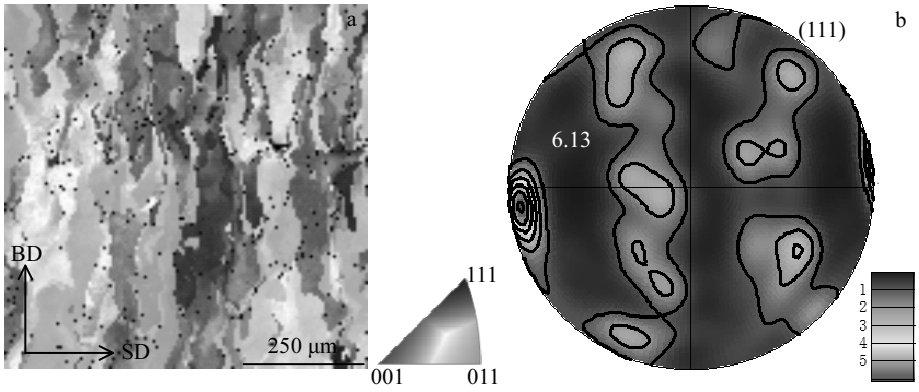

Fig.9 EBSD inverse pole figure image (a) and (111) pole figure (b) of the side-view of the SLMed Ta sample

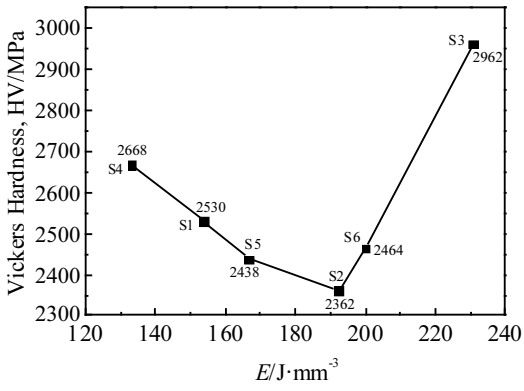

Fig.10 Microhardness of SLMed Ta samples under different processing parameters

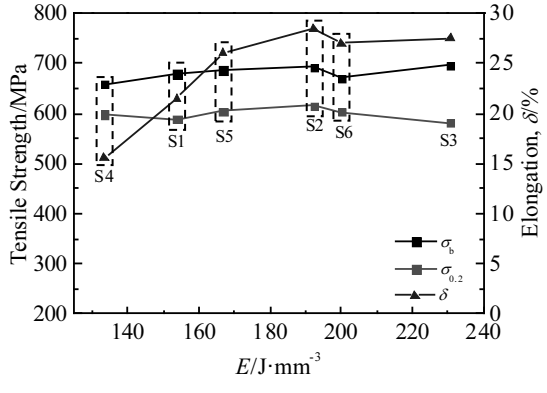

Fig.11 Tensile strength and elongation variation with the energy density

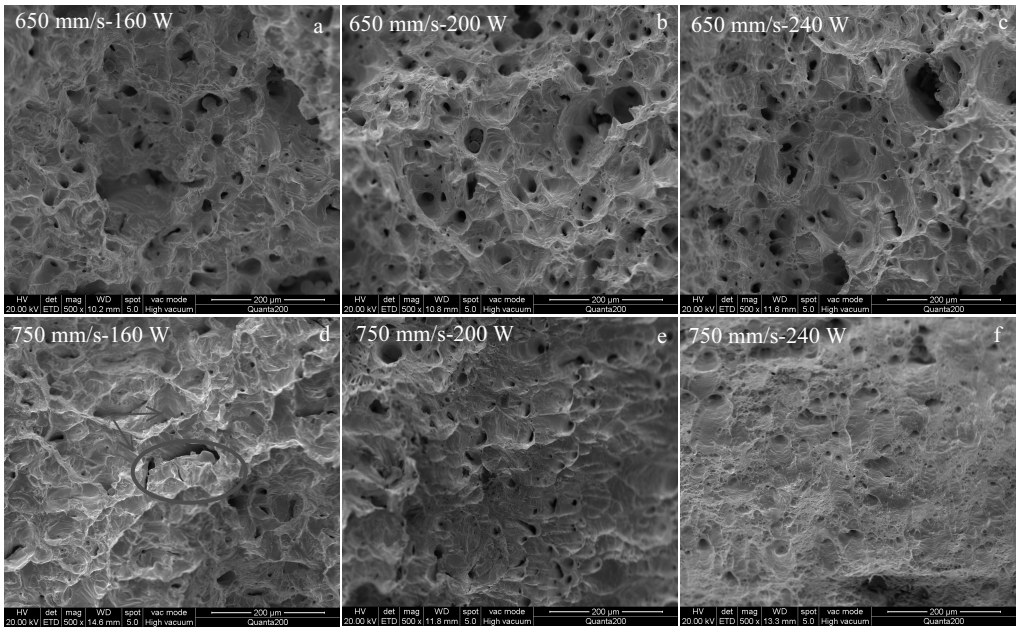

Fig.12 Tensile fracture morphologies of the SLMed Ta samples using different processing parameters: (a) v=650 mm/s, P=160 W; (b) v=650 mm/s, P=200 W; (c) v=650 mm/s, P=240 W; (d) v=750 mm/s, P=160 W; (e) v=750 mm/s, P=200 W; (f) v=750 mm/s, P=240 W

work[18], the tensile strength is not sensitive to the energy density change. The minimum and maximum ultimate tensile strengths are achieved at 659 and 697 MPa at the energy density of 133.33 and 230.77 J/mm^3, respectively. It is remarkable that the elongation to failure of the SLMed Ta samples is significantly improved in comparison with the results obtained by Zhou et al[18]. The maximum elongation can reach ~28.5% in the sample S2, which is comparable to the pure Ta fabricated using powder metallurgy method[15]. It should be noted that in the previous studies, pure Ta usually possess large elongation at the expense of the strength. For example, Ta fabricated by powder metallurgy method with the elongation of 30% only has an ultimate tensile strength of 310 MPa[15]. However, in the current study, the large elongation and the high tensile strength are achieved at the same time. These improved mechanical properties can be also attributed to the extraordinary densification owing to the spherical powder manufactured using radio frequency plasma spheroidization system. In addition, the oxygen content of the raw powder is as low as 481 μL/L. The low oxygen concentration in the raw material and the protection Ar atmosphere in the SLM process ensure little oxidation detriment effect on the ductility[30].

Fig.12 shows the microscopic fracture morphologies of the SLMed Ta samples. Combined with Fig.11, it can be seen that in the sample with the lowest elongation (S4), pores are present on the fracture surface, as indicated by the ellipse in Fig.12d. The pores form due to the insufficient laser energy deposition, and it is in agreement with its low relative density (Fig.3). In addition, some cleavage facets are found on the fracture surface, as indicated by arrows in Fig.12d, which are also responsible for the relatively low elongation. In other samples, a large number of micro-sized dimples are observed, which suggest that the SLMed Ta samples possess good ductility.

3 Conclusions

1) The microstructure and mechanical properties of tantalum produced by selective laser melting (SLM) using radio frequency plasma spheroidized powder are investigated under different processing parameters. At a fixed scanning speed, the relative density increases with the laser power. A fully dense sample with a relative density of 99.96% can be obtained at the scanning speed of 650 mm/s and the laser power of 240 W. Compared to the powder with irregular shape, the densification behavior and surface smoothness can be greatly improved using spherical powder. A strong preferred orientation of <111> parallel to the building direction is developed in the SLMed Ta sample.

2) The microhardness peak value of 2962 MPa is obtained for the fully dense sample, and the maximum values of the ultimate tensile strength and the elongation reach 697 MPa and 28.5%, respectively.

References

1 Fulcher O H. *Journal of the American Medical Association*[J], 1943, 121(12): 931

2 Panjaitan B, Noviana D, Gunanti *et al*. *Advanced Materials Research*[J], 2015, 1112: 470

3 Yang Hailin, Li Jing, Zhou Zhongcheng *et al*. *Materials Letters*

[J], 2013, 100: 152
4 Balla V K, Bodhak S, Bose S *et al*. *Acta Biomaterialia*[J], 2010, 6(8): 3349
5 Chen Changjun, Zhang Min. *Advanced Materials Research*[J], 2012, 476-478: 2063
6 Stiehler M, Lind M, Mygind T *et al*. *Journal of Biomedical Materials Research Part A*[J], 2008, 86(2): 448
7 Fathi M H, Azam F. *Materials Letters*[J], 2007, 61(4): 1238
8 Shi Liangyu, Wang An, Zang Fazhi *et al*. *Colloids Surf B: Biointerfaces*[J], 2017, 160: 22
9 Ding D, Xie Y, Li K *et al*. *Materials*[J], 2018, 11(4): 546
10 Moon B H, Choe H C, Brantley W A. *Applied Surface Science*[J], 2012, 258(6): 2088
11 Kim W G, Choe H C, Ko Y M. *Advanced Materials Research*[J], 2007, 26-28: 821
12 Samuel S, Nag S, Nasrazadani S *et al*. *Journal of Biomedical Materials Research Part A*[J], 2010, 94(4): 1251
13 Wauthle R, Van Der Stok J, Yavari S A *et al*. *Acta Biomaterialia*[J], 2015, 14: 217
14 Livescu V, Knapp C M, Gray III G T *et al*. *Materialia*[J], 2018, 1: 15
15 Balla V K, Banerjee S, Bose S *et al*. *Acta Biomaterialia*[J], 2010, 6(6): 2329
16 Gibson I, Rosen D, Stucker B. *Additive Manufacturing Technologies*[M]. New York: Springer, 2010
17 Gu D D, Meiners W, Wissenbach K *et al*. *International Materials Reviews*[J], 2012, 57(3): 133
18 Zhou Libo, Yuan Tiechui, Li Ruidi *et al*. *Materials Science and Engineering A*[J], 2017, 707: 443
19 Gu D D, Hagedorn Y C, Meiners W *et al*. *Acta Materialia*[J], 2012, 60(9): 3849
20 Lee Y S, Zhang W. *Solid Freeform Fabrication Symposium*[C]. Austin: TX, 2015
21 Simchi A, Pohl H. *Materials Science and Engineering A*[J], 2003, 359(1-2): 119
22 Simchi A. *Materials Science and Engineering A*[J], 2006, 428(1-2): 148
23 Irrinki H, Jangam J S D, Pasebani S *et al*. *Powder Technology*[J], 2018, 331: 192
24 Qin Qun, Chen Guangxia. *Advanced Materials Research*[J], 2014, 834: 872
25 Liu Yang, Yang Yongqi, Wang Di. *The International Journal of Advanced Manufacturing Technology*[J], 2016, 87(1-4): 647
26 Mugwagwa L, Dimitrov D, Matope S *et al*. *Procedia Manufacturing*[J], 2018, 21: 92
27 Thijs L, Sistiaga M L M, Wauthle R *et al*. *Acta Materialia*[J], 2013, 61(12): 4657
28 Das M, Balla V K, Basu D *et al*. *Scripta Materialia*[J], 2010, 63(4): 438
29 Huang Y, Maury N, Zhang N X *et al*. *IOP Conference Series: Materials Science and Engineering*[M]. Bristol: IOP, 2014, 63: 12 100
30 Cramer S D, Covino J B S. *ASM Handbook*[M]. Ohio: ASM International Metals Park, 2003: 13A

选区激光熔化成形射频等离子体球化钽粉的微观组织与力学性能

施　麒[1,2,3]，毛新华[1,2,3]，谭　冲[1,2,3]，丁　超[1,2,3]，刘　辛[1,2,3]

(1. 广东省科学院 材料与加工研究所，广东 广州 510650)

(2. 国家钛及稀有金属粉末冶金工程技术研究中心，广东 广州 510650)

(3. 广东省金属强韧化技术与应用重点实验室，广东 广州 510650)

摘　要：采用射频等离子体球化法制备的球形钽粉进行选区激光熔化（SLM）成形致密化研究。通过工艺参数优化，在扫描速度为 650 mm/s 和激光能量为 240 W 条件下，获得了完全致密的钽样件。由于原始粉末具有较高的流动性，激光成形钽样件表现出较好的成形性能和表面质量。微观组织表征结果显示，样件顶面和侧面分别呈现等轴晶和柱状晶。EBSD 结果表明，在制造方向呈现<111>择优取向。最高显微硬度和抗拉强度分别达到 2962 和 697 MPa，致密样件的延伸率也显著提高到 28.5%。

关键词：选区激光熔化；球形钽粉；致密化；织构；力学性能

作者简介：施　麒，男，1987 年生，博士，广东省科学院材料与加工研究所，广东 广州 510650，电话：020-61086628，E-mail: shiqi@gimp.gd.cn